Some applications of seismogram synthesis through the summation of modes of Rayleigh waves

P. Suhadolc[1] and G.F. Panza[1,2]

[1] Istituto di Geodesia e Geofisica, Università di Trieste, Italy
[2] International School for Advanced Studies, Trieste, Italy

Abstract. Complete synthetic seismograms can be computed by the superposition of the fundamental and higher modes of Rayleigh waves. The usefulness of this approach is illustrated by the fact that it is possible to reproduce with sufficient detail experimental signals lasting several tens of seconds and having a high-frequency content (up to 1 Hz). The method has been proven to work even for higher frequencies, up to 10 Hz. To illustrate the source and structure modelling using this method, the whole experimental records from the Carder displacement meter at the station El Centro for the 1968 Borrego Mountain earthquake have been fitted. Seismic profiles (displacement, velocity and acceleration) have been synthesized and they clearly show the expected agreement between ray travel times and arrival times of different phases.

Key words: Synthetic seismograms – Modal summation – Borrego Mountain 1968 earthquake

Introduction

By summing the normal modes of a given structure, which approximates a certain region of the Earth with flat parallel layers (Panza, 1985), and using realistic models of a seismic source, it is possible to construct synthetic seismograms. The use of Rayleigh waves permits the modelling of the vertical and radial displacements; the use of Love waves, the transversal displacement. This approach has already been used with some success by Swanger and Boore (1978), referred to as SB hereafter, who used only four modes in the computation and did not include anelasticity.

In this article we demonstrate the efficiency and the power of the method using the summation of Rayleigh waves to fit experimental records. Another possibility, shown with a theoretical example, is to use such synthetics to interpret the data from deep seismic sounding experiments, in order to retrieve information regarding the S-wave velocity distribution not easily attainable with classical methods.

Theory

It was shown by Harkrider (1970), assuming a point double couple source model, that it is possible to represent the

Fourier transform of the displacement due to a Rayleigh mode by the following expressions:

$$U_r = R(\omega)\,|\mathbf{n}|\,k^{\frac{1}{2}}\exp(-i3\pi/4)\,x(\theta,h)$$
$$\cdot \varepsilon_0\,A\,\exp(-ikr)/(2\pi r)^{\frac{1}{2}}$$
$$U_z = [\varepsilon_0\,\exp(i\pi/2)]^{-1}\,U_r \tag{1}$$
$$U_t = 0$$

where $R(\omega)$ is the Fourier transform of the point-source time function, $\mathbf{n}$ is the unit vector perpendicular to the fault plane and has units of length, k is the wavenumber, r is the epicentral distance, $x(\theta,h)$ represents the azimuthal dependence of the source radiation which contains the fault-plane parameters and the eigenfunctions at the source depth, ε_0 is the ellipticity and $A = (2cUI_1)^{-1}$ with c, U and I_1 the phase velocity, group velocity and energy integral, respectively (see Panza et al., 1973 for details). The factor $(2\pi r)^{-\frac{1}{2}}$ comes essentially from the first term of the asymptotic expansion of the Hankel function. This approximation, together with neglecting terms of higher order in $r^{-\frac{1}{2}}$, enables results to be obtained with at least three significant figures whenever $kr > 10$ (Panza et al., 1973).

The attenuation is included by making k complex (e.g. Panza, 1985). Causality is preserved by introducing the body-wave dispersion according to Futtermann (1962).

In these computations we deliberately neglect the contribution of the branch line integral corresponding to the half-space. This may have some effect on the P-wave arrivals from layers with compressional wave velocity close to or larger than the S-wave velocity in the half-space (Harvey, 1981). However, the capability of handling large quantities of structure enables the synthesis of most arrivals from crustal layers (Panza, 1985).

Examples of the computation of the quantities which appear in Eq. (1) are given by Panza (1985). In this article we will be dealing with time-domain computations. A main advantage of the mode summation compared with other existing methods for the construction of synthetic seismograms described elsewhere in this volume, apart from the relatively easy way to treat anelasticity and the use of a great number of layers, is the following. All the factors in Eq. (1), with the exception of $x(\theta,h)$, are independent of the source mechanism and need therefore be computed only once. The earth response for every distance and for an arbitrary mechanism can be quickly computed by a simple inverse Fourier transform, summed over the modes.
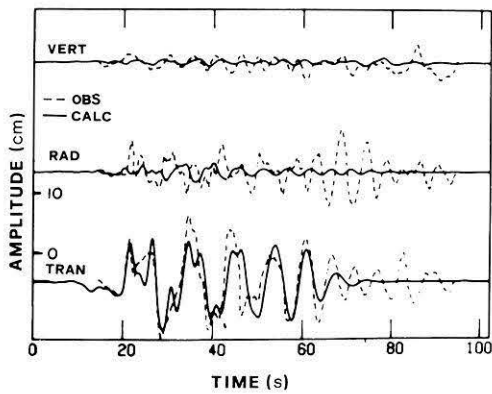
Fig. 1. Vertical, radial and transversal component of the observed displacement (*dashed*) and synthetic displacement for a point source (*continuous*) of the Borrego Mountain, California, 1968 earthquake (after Swanger and Boore, 1978). The station is El Centro

Synthetic seismograms

To show the validity of our computer program for the summation of Rayleigh wave modes, we tried to reproduce the recordings of the Carder displacement meter of the Borrego Mountain, California, earthquake of April 9, 1968 (Heaton and Helmberger, 1977, referred to as HH hereafter).

An attempt to model this earthquake in terms of summation of surface-wave modes has been done by SB. These two authors were able to reproduce the transversal component of motion quite well, but failed to obtain a good fit for the radial and vertical component (Fig. 1). We have therefore tried to fit these two components in order to test our computer program.

The initial structure used in the computations is shown in Fig. 2a. The crustal structure, Fig. 2b, is taken from the structure used by SB. The mantle part is taken from the models proposed by Biswas and Knopoff (1974) for the western United States.

In the initial step of fitting the radial component, we held the structure fixed and varied only some of the source parameters. At the beginning we used a single-point-source model, while later on a two-point model is shown to give a better fit.

Single-point source

The radial component of the observed seismogram is shown in Fig. 3a. For the source parameters, we adopted those given by Burdick and Mellman (1976). These authors modelled the teleseismic P pulse by adding the contribution of three point sources occurring in a time span of about 15 s. We used the parameters of the first of these three events, which are also in good agreement with the values proposed by Allen and Nordquist (1972). A Heaviside step function was used for the source time function.

The synthetic seismogram obtained with these parameters and the sum of 218 modes is shown in Fig. 3b. For a unitary seismic moment, the zero-to-peak amplitude of the synthetic of Fig. 3b is 6.1×10^{-26} cm. To obtain the observed maximum displacement we need a seismic moment of about 12×10^{25} dyne-cm.

It is evident that the coda amplitudes of the observed seismogram are much larger than those of the synthetic.
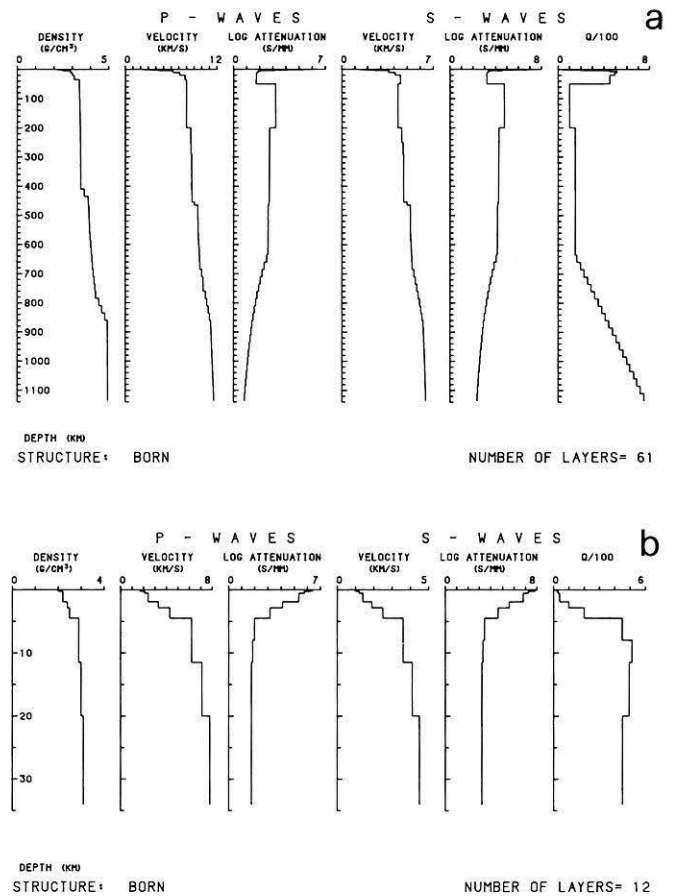
Fig. 2. a BORN structure used to construct the synthetic seismograms of Figs. 3b, 4a, 4b, 5. **b** BORN structure, crustal part
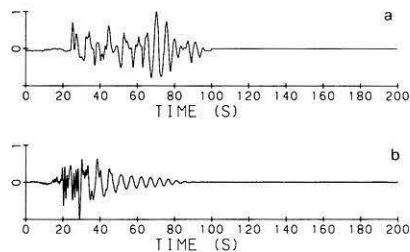
Fig. 3. a Observed radial component of the ground motion due to the Borrego Mountain, California, 1968 earthquake, recorded at El Centro station. Maximum zero-to-peak amplitude is about 7.3 cm. **b** Synthetic seismogram: radial component, point source, $r = 66$ km, $h = 8$ km, strike $= 185°$, dip $= 81°$, rake $= 178°$, source duration $= 0$ s, summed modes $= 218$, $M_0 = 12 \times 10^{25}$ dyne-cm, structure BORN. Unless explicitly specified, the parameters of the synthetic seismograms in the other figures are the same as those of this figure. The reported values of M_0 are obtained by scaling the maximum zero-to-peak amplitude of the 1 dyne-cm synthetics to the observed one

This problem may be removed by a variation in the depth of the source, which greatly affects the relative amplitudes between the early and late parts of the recording. The large-amplitude late arrivals could not be explained, according to SB. HH, on the other hand, attribute them to lateral reflections and refractions from the edges of the Salton Trough, the structural depression underlain and bounded
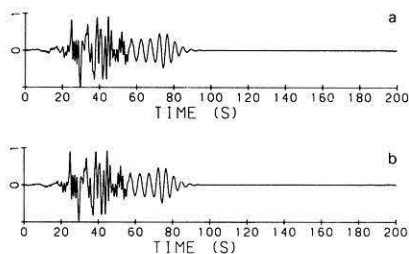
Fig. 4. a Synthetic seismogram: $h = 4.5$ km, $M_0 = 9 \times 10^{25}$ dyne-cm. **b** Synthetic seismogram: $h = 4.5$ km, summed modes = 13, $M_0 = 9 \times 10^{25}$ dyne-cm

Fig. 6. Structure BORD. Only the crustal part is shown, the mantle part coincides with that of structure BORN
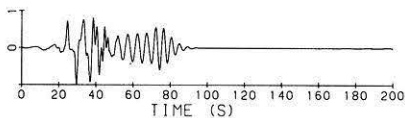
Fig. 5. Synthetic seismogram: $h = 4.5$ km, source duration = 2 s, $M_0 = 13 \times 10^{25}$ dyne-cm

Fig. 7. Synthetic seismogram: $h = 4.5$ km, source duration = 2 s, summed modes = 13, $M_0 = 13 \times 10^{25}$ dyne-cm, structure BORD

by crystalline rocks and filled with sediments, in which both the epicentre and receiver lie. A simple way to obtain them is, as said above, by a shallower source. The synthetics obtained with a source depth of 4.5 km, and leaving the other parameters the same, is shown in Fig. 4a. Some significant improvement is evident. The stronger excitation of Rayleigh waves in the sedimentary surficial layers, which is probably responsible for the high-amplitude late arrivals, is accomplished by a shallower source.

Before going on, by varying source and structure parameters, we note that for this distance the main contribution to the seismogram is given by the lower modes. The effect of higher modes is to better approximate the initial part of the seismogram and the first arrivals in particular. In order to save computing time, and work therefore almost interactively, we decided to sum from 5 to 13 modes only in our trial-and-error procedure to fit the actual recording. To show that this is in fact reasonable, the synthetic in Fig. 4b is computed with exactly the same parameters as that in Fig. 4a, but now summing only 13 modes instead of 218. The difference between the two is almost unnoticeable.

The high frequencies present in the early arrivals of the synthetic seismogram of Fig. 4a can be filtered out by using a finite rise-time source function. We adopted a symmetric triangular function for the derivative of the source time function. The resulting synthetic, for a duration of 2 s, is shown in Fig. 5.

The principal difference seen between the synthetic and the observed recording is still in the amplitudes. The amplitudes of the later arrivals dominate in the observed recording, while in the synthetic the early arrivals are the larger ones.

To further reduce the ratio between the early and later arrivals we tried to increase the Q factor in the sediments and to diminish it in the crust, as shown in Fig. 6. The structure BORD is therefore similar to BORN apart from the Q values in the first seven layers. A small improvement is seen in the corresponding synthetic given in Fig. 7.

For a better fit, some structural parameters have to be changed. In particular, we note that the frequency of the fundamental mode, which produces the large-amplitude
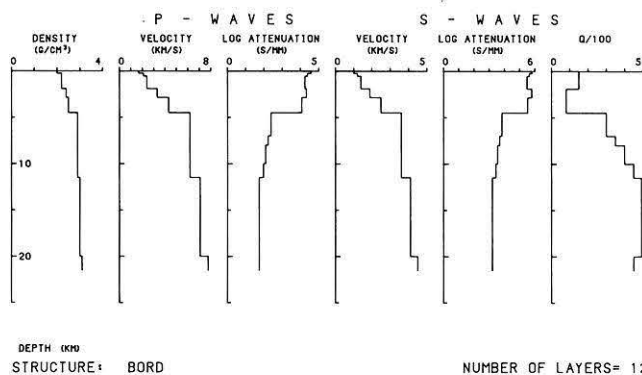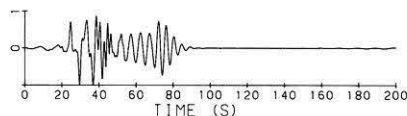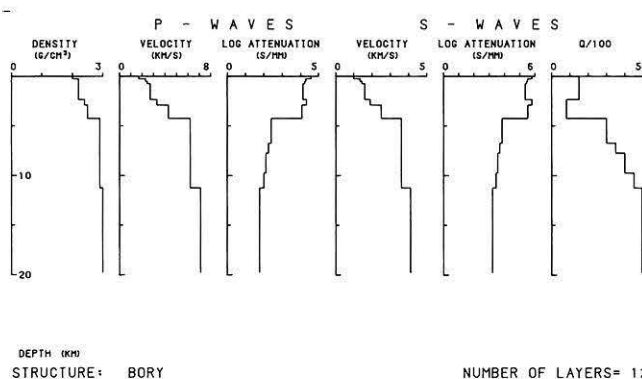
Fig. 8. Structure BORY. Only the crustal part is shown, the mantle part coincides with that of structure BORN

later arrivals, is lower in the observed seismogram than in the synthetic one. This can be taken care of by increasing the thicknesses of the uppermost layers. After some trials in adjusting the corresponding velocities in order to maintain the correct arrival times, the structure shown in Fig. 8 was found to give the best results. The corresponding synthetic, for a source duration of 3 s, a value used also by SB, is given in Fig. 9a. The fit in the later arrivals is now quite good. The corresponding seismic moment is about 9×10^{25} dyne-cm, in good agreement with the values given by SB and HH.

The discrepancies which still persist between observed and synthetic data are in the large early arrivals, the initial double peak and the latest arrival, which have not been synthetised up till now. The problem can be resolved by considering more than one point source.

Two-point sources

An easy way to reduce the amplitudes of the first arrivals is to consider more than one point source. HH and Burdick and Mellman (1976) also find that the event cannot be
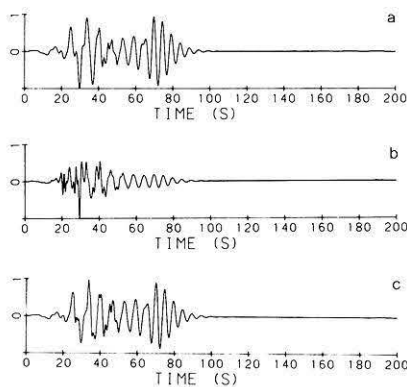
Fig. 9. a Synthetic seismogram: $h = 4.5$ km, source duration $= 3$ s, summed modes $= 218$, $M_0 = 9 \times 10^{25}$ dyne-cm, structure BORY. **b** Synthetic seismogram: $h = 8$ km, source duration $= 1$ s, summed modes $= 218$, $M_0 = 5 \times 10^{25}$ dyne-cm, structure BORY. **c** Synthetic seismogram: two-point-source event, the two point sources correspond to those of Figs. 9a and b. The two sources are given equal weight, the deeper one being delayed 6 s with respect to the shallower one. Total $M_0 = 11 \times 10^{25}$ dyne-cm
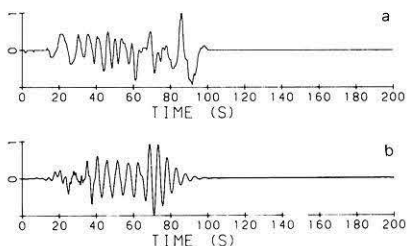
Fig. 10. a Observed vertical component of the ground motion due to the Borrego Mountain, California, 1968 earthquake, recorded at El Centro station. Maximum zero-to-peak amplitude is about 3.1 cm. **b** Synthetic seismogram: vertical component, $M_0 = 5 \times 10^{25}$ dyne-cm, structure BORY, two-point-source event corresponding to that of Fig. 9c

Fig. 11. Synthetic profile: displacements, for a strike-slip source with unitary seismic moment ($M_0 = 1$ dyne-cm), maximum frequency 1 Hz, structure BORN. The travel times for the distance of 120 km and *from left to right* are: refracted P_1 and refracted P_2 (superposed), reflected P_2, reflected P_1, refracted S_1 and refracted S_2 (superposed), reflected S_2, direct P, reflected S_1, direct S. (The subscripts 1 and 2 indicate the reflection and refraction with respect to the interfaces at 11.5 km and 20 km, respectively, see Fig. 2b)

modelled with a single point source. In order to preserve the good-fitting later arrivals and change only the early part of the synthetic, a second deeper point source is considered. Since the early arrivals show more high-frequency content, a source 8 km deep with a time duration of 1 s was chosen. The seismogram is shown in Fig. 9b. The effect on station El Centro (ELC) of the two point sources, the deeper one being 6 s late with respect to the shallower one, is shown in Fig. 9c. The weights of the two point sources were chosen to be identical, resulting in a total seismic moment of about 10×10^{25} dyne-cm.

The other features could probably be modelled assuming more point sources located at different hypocentres, but the problem has not been dealt with in this paper, since it is not our aim to make a particular study of the Borrego Mountain event.

The synthetic vertical component (the observed vertical component is shown in Fig. 10a) corresponding to the synthetic of Fig. 9c is given in Fig. 10b. The overall fit is not bad at all, especially in the middle part of the record, but the latest arrivals of the observed recording show sharp phase changes and very large periods and amplitudes, features missing in the synthetics of Fig. 10b. These are very probably due to the interference effect of more point sources.

At this stage, however, we consider any further attempt to model this component useless since its size, only about one third of the radial, is just above the noise level.

An extended source can also be tried with our program by approximating each square kilometre, say, of the fault surface with a point dislocation source. Without entering into the question of the faulting process and not claiming to have improved on previous workers, we just note that our modelling confirms the complexity of the source of seismic energy.

We have, therefore, shown that our computer program based on the summation of surface-wave modes is quite versatile and can be used to model observed recordings in a highly realistic way.

Synthetic profiles

In this section we consider a single point source with an instantaneous dislocation of the strike-slip type and the structural model of Fig. 2. An example with an explosive source is treated in Suhadolc and Marson (1985).

By varying only the distance from the source, it is possible to construct synthetic seismic profiles in an easy way. These can be utilized to interpret the observed profiles in deep seismic sounding experiments with obvious but substantial advantages with respect to the techniques currently
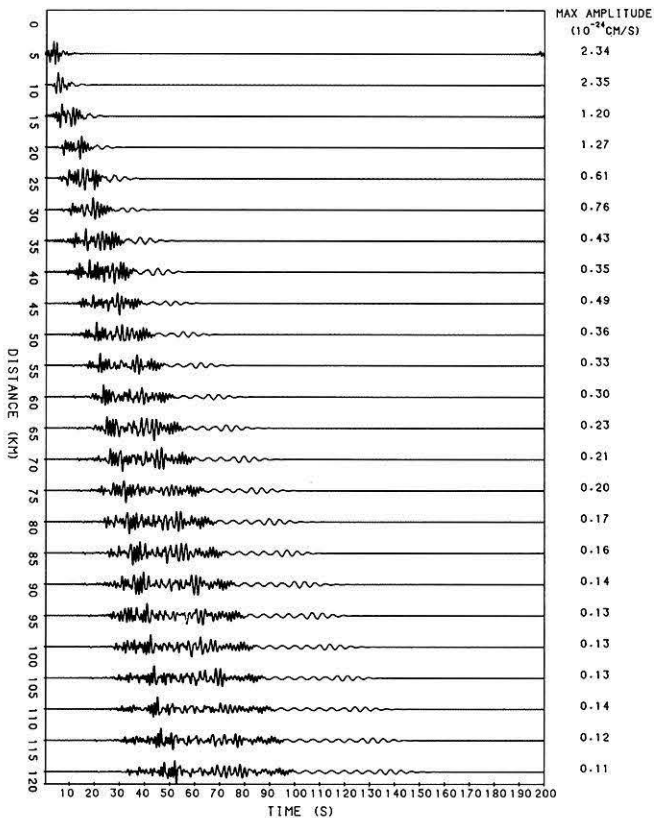
Fig. 12. Synthetic profile: velocities, maximum frequency 1 Hz, structure BORN. Same source as in Fig. 11
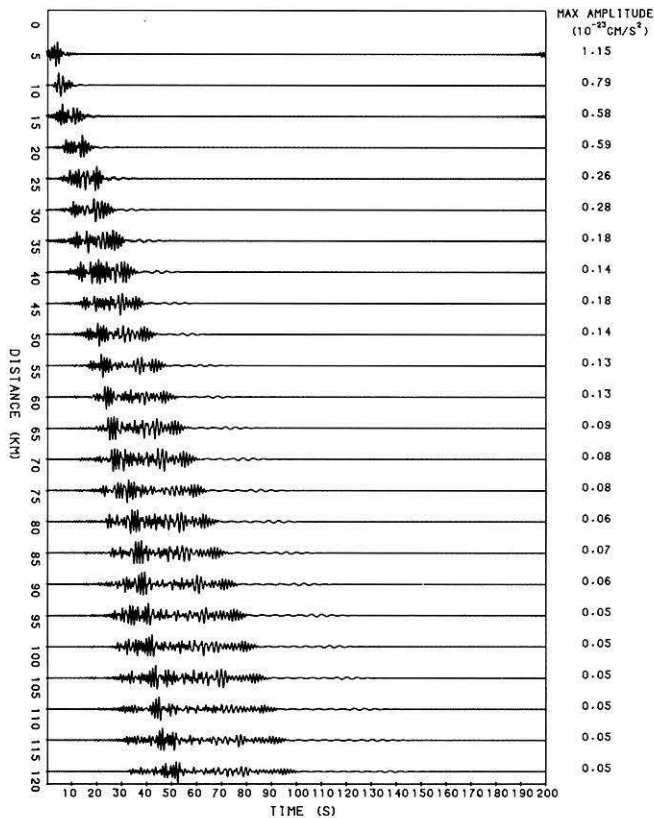
Fig. 13. Synthetic profile: accelerations, maximum frequency 1 Hz, structure BORN. Same source as in Fig. 11

in use. An example of such a profile is given in Fig. 11. On the figure, some travel-time curves are drawn.

The correlation between the phases which could be seen on the seismograms and the travel-time curves, which were computed with ray theory, is quite good. Note the expected small amplitude, with respect to the dominant phases of the seismogram (S waves), of the refracted and reflected P waves. The various phases arriving before and after the direct S wave, which are not interpreted in Fig. 11, correspond to multiple reflections in the sedimentary layers. For example, the prominent phase at about 48 s at 120 km corresponds to a multiple reflection in the sedimentary layer just above the basement.

We have computed displacements up till now. It is also possible, however, to compute velocities and accelerations by simply multiplying the results of Eq. (1) by $i\omega$ and $-\omega^2$, respectively. In general it is also possible, with a simple convolution, to obtain the signal corresponding to the output of a general instrument with known characteristics. Examples of velocity and acceleration profiles corresponding to the displacement profile of Fig. 11 are given in Figs. 12 and 13.

Since the frequencies involved in experimental refraction profiles are larger than 1 Hz, we performed some computations up to 10 Hz. In this case we used lithospheric structures, i.e. structures with elastic and anelastic characteristics specified down to a depth of about 40 km. The structure used, BOR 1, is given in Fig. 14a and the synthetic seismogram corresponding to a point source with a prevailing dip-slip mechanism at a distance of 10 km is shown in Fig. 14b. On the figure, an interpretation based on ray theory of some phases is given. In our notation, the sub-
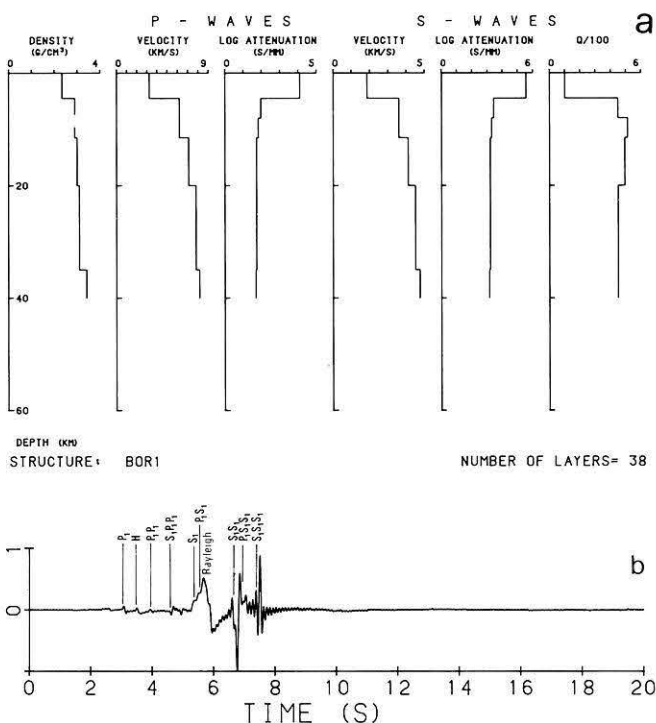
Fig. 14. a Structure BOR 1 used to construct the seismogram shown in Fig. 14 b. **b** Synthetic seismogram: displacement, vertical component, $r=10$ km, $h=1$ km, strike $=254°$, dip $=25°$, rake $=280°$, source duration $=0$ s, $M_0 = 1$ dyne-cm, maximum zero-to-peak amplitude $=6.1 \times 10^{-23}$ cm, maximum frequency 10 Hz, structure BOR 1. Some of the phases are interpreted with ray theory (the subscript 1 indicates propagation in the first layer)
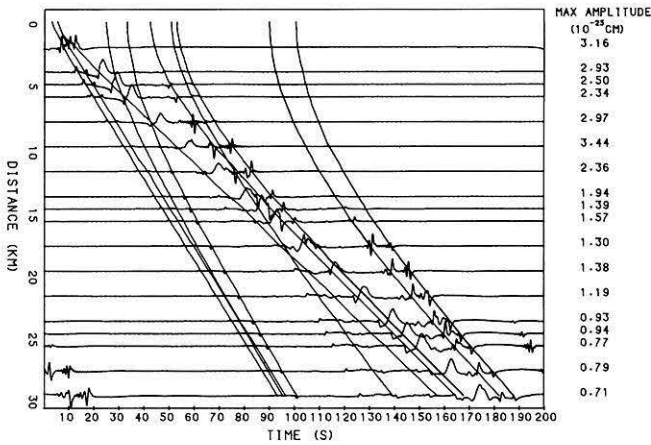
Fig. 15. Synthetic profile: displacements, same source as in Fig. 14b, maximum frequency 10 Hz, structure BOR 1. The travel-time curves at the distance of 10 km correspond to the arrival times given in Fig. 14b. For greater times, two more curves are shown which correspond to the multiple reflections of the S wave in the first layer ($S_1 S_1 S_1 S_1$ and $S_1 S_1 S_1 S_1 S_1$). For distances greater than about 25 km a time-domain aliasing phenomenon is seen

script indicates the layer in which the wave propagates; thus, for example $P_1 S_1$ is a wave starting as P and reaching the receiver after being reflected as S at the bottom of layer 1. As can be seen, the agreement is very good not only for direct waves and simple reflections, but also for the surface head wave H, the converted phases and the multiple S reflections in the surficial layer.

Due to the above result, we also synthesized a profile for frequencies up to 10 Hz, and the result is shown in Fig. 15. The travel-time curves are those corresponding to some of the phases interpreted in Fig. 14b. The last two curves correspond to the multiple reflections $S_1 S_1 S_1 S_1$ and $S_1 S_1 S_1 S_1 S_1$ in the surficial layer. For distances larger than about 25 km, an aliasing problem is present which can, however, be easily taken care of by interpolating the frequency spectrum.

Conclusions

It has been shown that the summation of modes of Rayleigh waves allows us to model, very efficiently and in a highly realistic way, the observed ground motions due to earthquakes. The radial component of the ground motion of the Borrego Mountain 1968 earthquake recorded at El Centro station, California, has been quite successfully modelled. Complete synthetic seismograms (displacements, velocities and accelerations) obtained in this way and arranged in a seismic profile show an excellent agreement between theoretical travel times computed with ray theory and the main phases on the seismogram.

References

Allen, C.R., Nordquist, J.M.: Foreshock, main shock and larger aftershocks of the Borrego Mountain earthquake. U.S. Geol. Surv. Profess. Paper **787**, 16–23, 1972

Biswas, N.N., Knopoff, L.: The structure of the upper mantle under the United States from the dispersion of Rayleigh waves. Geophys. J.R. Astron. Soc. **36**, 515–539, 1974

Burdick, L.J., Mellman, G.R.: Inversion of the body waves from the Borrego Mountain earthquake to the source mechanism. Bull. Seismol. Soc. Am. **66**, 1485–1499, 1976

Futtermann, W.I.: Dispersive body waves. J. Geophys. Res. **67**, 5279–5291, 1962

Harkrider, D.G.: Surface waves in multilayered elastic media. Part II. Higher mode spectra and spectral ratios from point sources in plane layered earth models. Bull. Seismol. Soc. Am. **60**, 1973–1987, 1970

Harvey, D.J.: Seismogram synthesis using normal mode superposition: the locked mode approximation. Geophys. J.R. Astron. Soc. **66**, 37–69, 1981

Heaton, T.H., Helmberger, D.V.: A study of the strong ground motion of the Borrego Mountain, California, earthquake. Bull. Seismol. Soc. Am. **67**, 315–330, 1977

Panza, G.F.: Synthetic seismograms: the Rayleigh waves modal summation. J. Geophys. 1985

Panza, G.F., Schwab, F., Knopoff, L.: Multimode surface waves for selected focal mechanisms. I. Dip-slip sources on a vertical fault plane. Geophys. J.R. Astron. Soc. **34**, 265–278, 1973

Suhadolc, P., Marson, I.: The use of synthetic seismograms in the profile interpretation: an example from Friuli, Italy. Terra Cognita **5**, 300, 1985

Swanger, H.J., Boore, D.M.: Simulation of strong-motion displacements using surface-wave modal superposition. Bull. Seismol. Soc. Am. **68**, 907–922, 1978